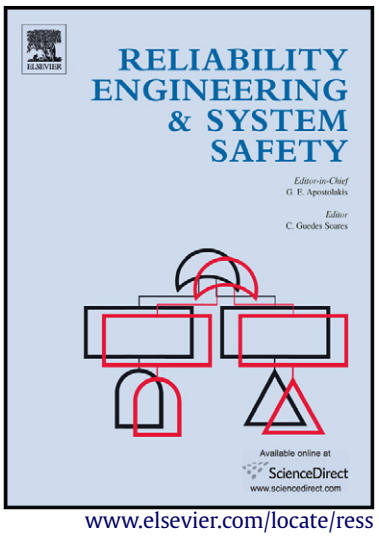

www.elsevier.com/locate/ress

Resilience Assessment of Interdependent Infrastructure Systems: With a focus on Joint Restoration Modeling and Analysis

Min Ouyang, Zhenhua Wang

PII: S0951-8320(15)00069-1
DOI: http://dx.doi.org/10.1016/j.ress.2015.03.011
Reference: RESS5259

To appear in: *Reliability Engineering and System Safety*

Received date: 28 April 2014
Revised date: 17 January 2015
Accepted date: 5 March 2015

Cite this article as: Min Ouyang, Zhenhua Wang, Resilience Assessment of Interdependent Infrastructure Systems: With a focus on Joint Restoration Modeling and Analysis, *Reliability Engineering and System Safety,* http://dx.doi.org/10.1016/j.ress.2015.03.011

Resilience Assessment of Interdependent Infrastructure Systems: with a focus on Joint Restoration Modeling and Analysis

Min Ouyang[1], Zhenhua Wang[2]

Abstract: As infrastructure systems are highly interconnected, it is crucial to analyze their resilience with the consideration of their interdependencies. This paper adapts an existing resilience assessment framework for single systems to interdependent systems and mainly focuses on modeling and resilience contribution analysis of multi-systems' joint restoration processes, which are seldom addressed in the literature. Taking interdependent power and gas systems in Houston, Texas, USA under hurricane hazards as an illustrative exmaple, five types of joint restoration stategies are proposed, including random restoration strategy RS_1, independent restoration strategy RS_2, power first and gas second restoration strategy RS_3, gas aimed restoration strategy RS_4, and power and gas compromised restoration strategy RS_5. Results show that under limited restoration resources, RS_1 produces the least resilience for both systems, RS_2 and RS_3 both generates the largest power system resilience while RS_4 is the best for the gas system; and if quantifying the total resilience as the evenly weighted sum of two systems' individual resilience, RS_5 produces the largest total resilience. The proposed method can help decision makers search optimum joint restoration strategy, which can significantly enhance both systems' resilience.

Key words: Infrastructure Systems; Interdependencies; Resilience assessment; Cascading failures; Restoration; Genetic algorithm

[1] Associate Professor, Department of Systems Science and Engineering, Huazhong University of Science and Technology Wuhan, 430074 China; Key Laboratory of Image Information Processing and Intelligent Control (Huazhong University of Science and Technology), Ministry of Education, China; Email: min.ouyang@hust.edu.cn
[2] PHD candidate, Department of Civil and Environment Engineering, Rice University; 6100 Main Street, MS-318, TX 77005, United States; Email: zw8@rice.edu

1. Introduction

Scholars and governments in the field of disaster mitigation have paid many efforts to make communities and cities more "disaster-resilient" [1-4]. To improve the overall resilience of a community or a city, it is crucial to analyze resilience by focusing on infrastructure systems, which form the backbone for its functioning and provide essential services to support the well-being of its citizens in the aftermath of disruptive events. These critical facilities include electric power, water supply, telecommunication, emergence service systems and so on. However, these systems are not isolated but highly interconnected and mutually interdependent [5-7]. Interdependencies can improve infrastructure operational efficiency, but they can also increase system vulnerability, i.e., small failures in one infrastructure system can result in cascading failures within it and across other systems, largely impacting the regional or national economic systems as well as people's life. Hence, it is necessary to study infrastructure resilience with the consideration of their interdependencies, which is seldom addressed in the literature and will be then discussed in this work. As this paper is based on an existing resilience framework for single systems, this paper will next briefly review this framework and then introduce additional requirements for interdependent systems' resilience assessment as well as pertinent literature review.

In previous work [22], it defined resilience of an infrastructure system as its joint ability to *resist* (prevent and withstand) any possible hazards, *absorb* the initial damage, and *recover* to normal operation. Compared with other definitions in the literature [8-12], this definition can reflect systems' ability to reduce some events' frequencies. Based on this definition, the authors further introduced a time-dependent infrastructure resilience

metric and its assessment framework, which not only adequate for both single and multiple hazards [22-23], but also adequate for quantifying potential future resilience with the consideration of system evolution [24]. This metric is based on two curves during a time period: one is the real performance curve, recording system performance change under disruptive events and under restoration efforts, while the other is the targeted performance curve, giving system performance levels in the case of no disruptive event. The resilience value is then quantified as the ratio of the area between the real performance curve and the time axis during the period to the area between the target performance curve and the time axis during the period. The difference between this metric and other resilience metrics in the literature, such as the loss of resilience quantified as the area between the targeted performance curve and the real performance curve within the restoration period [13-14], a normalized shaded area underneath the performance curve of systems in a disruptive event [16-17], and some others [15, 18-21], is that the proposed metric is defined during a given period while others are defined for specific events during a specific restoration period without incorporating the event frequency. This paper will still use this time-dependent metric to assess the resilience of interdependent systems.

When applying that time-dependent resilience concept to interdependent systems, it requires system performance curves during a time period T with possible disruptive events, which means that it needs modeling and simulation of cascading failures across multiple systems and multi-systems' joint restoration processes under disruptive events. There exist many approaches to address these issues in the literature [25], such as empirical approaches, agent based approaches, system dynamics based approaches,

economic theory based approaches, network based approaches, and others. However, most of existing interdependency-related studies by these approaches mainly focused on the cascading failures within and across multiple systems to estimate system-level damage or vulnerability, with only a few addressing the restoration processes.

Some economic theory based studies modeled each infrastructure system by its industry sector in an economy system, and adapted the Leontief dynamic Input-output model for economic systems to describe the recoveries of infrastructure systems (or industry sectors) following a disruptive event. Based on the initial perturbations of sectors caused by the event and on the estimated recovery times, the adapted model could calculate the inoperabilities and economic losses of interdependent sectors during the recovery period [26-27]. However, this system-level model cannot model decision makings at infrastructure component level, such as restoration sequence of damaged components, and mobilization of restoration resources during the restoration period. To model these restoration details, Wallace and Lee [28-29] modeled different infrastructure functionality by a uniform network flows mathematical representation and then analyzed the multi-systems' restoration processes by solving a flow optimization problem. However, different types of infrastructure systems are all modeled by a maximum network flow model is unrealistic; for some systems, taking power systems as examples, if modeled by a maximum network flow model, it could produce large different vulnerability results under disruptive events from those realistic models [30-31], such as direct current power flow model. Recently Coffrin et al. addressed the restoration problem of interdependent power and gas system by modeling the former by a direct current power flow model and the latter by a maximum network flow model, and then

analyzed multi-systems' restoration processes by solving a Mix integer programming model to maximize the weighted sum of interdependent demand during the whole restoration period [32]. However, this model did not consider various repair times for damage components and different quantities of restoration resources. This paper will address these features and propose a multi-systems' joint restoration model to support interdependent systems' resilience assessment.

The rest of this paper is organized as follows: Section 2 introduces the resilience assessment framework for interdependent systems, with a focus on modeling of multi-systems' joint restoration processes. Section 3 takes the interdependent power and gas systems in Harris County, Texas, USA under hurricane hazards as an example to illustrate the proposed resilience method and mainly discusses resilience contribution of various restoration strategies. The last Section 4 provides the discussions and conclusions of this study and includes directions for future research.

2. Resilience Assessment Framework of Interdependent Infrastructure Systems

The resilience metric is built upon the system performance process during a time period from 0 to T [22-24], which may include none or several disruptive events, as shown in Fig. 1. Each event covers a disaster prevention stage ($t_0 \le t \le t_1$), a damage propagation stage ($t_1 < t \le t_2$) and an assessment and recovery stage ($t_2 < t \le t_3$). These three stages can respectively reflect resistant, absorptive and restorative capacities of the system under that event, and these capacities reflected from 0 to T together determine system resilience over that time horizon. Resilience is then quantified according to the targeted performance curve $P_T(t)$ and the real performance curve $P_R(t)$:

$$R(T) = \int_0^T P_R(t)dt \Big/ \int_0^T P_T(t)dt \tag{1}$$

Note that different periods T yield different forms of resilience: *previous resilience*, *current potential resilience* and *future potential resilience* [24]. This paper mainly investigates the current potential resilience, where system parameters are fixed during 0 to T and equal to those at the current time. For the case in which the current potential resilience $P_T(t)$ is a constant value 1.0, and when a hazard of interest has its occurrence governed by a Poisson process [22], the expected resilience $E[R(T)]$ is:

$$E[R(T)] = E\left[\frac{\int_0^T P_R(t)dt}{T}\right] = E\left[\frac{T - \sum_{n=1}^{N(T)} IA_n(t_n)}{T}\right] = 1 - E\left[\frac{1}{T}\sum_{n=1}^{N(T)} IA_n(t_n)\right] \tag{2}$$
$$= 1 - \frac{1}{T}\sum_{N=0}^{\infty} N \times E[IA]\frac{(\lambda T)^N e^{-\lambda T}}{N!} = 1 - \lambda E[IA]$$

where $E[\bullet]$ is the expected value; n is the event occurrence number; $N(T)$ is the total number of event occurrences during T; t_n is the occurrence time of the n-th event, which is a random variable; $IA_n(t_n)$ is the area between the real performance curve and the targeted performance curve, called impact area for the n-th event occurrence at time t_n; $E(IA)$ is the expected impact area under the hazards accounting for all possible intensities; and λ is the occurrence rate of the hazards per year. Clearly, Eq. (2) indicates that the current potential resilience has an expected value not related with T.

Based on the above resilience metric, this paper will take the power system and the gas system in Harris County, Texas [33] as an example to illustrate a network-based framework for interdependent systems' resilience assessment. This framework includes four steps: descriptions of single systems and their interdependencies, modeling of

hazards and component fragilities, modeling of cascading failures within and across infrastructure systems, and modeling of multi-systems' restoration processes. Note that the first three steps are the procedures for interdependent system vulnerability analysis and have been studied for the two systems in the previous work [23, 34], then this section will briefly introduce them, with a focus on the forth step.

2.1 Descriptions of single infrastructure systems and their interdependencies

This paper uses a network-based approach to describe single systems and their interdependencies. For the gas system in Harris County, the gas compressors, the gas storage facilities, the gas delivery facilities, the gas receipt facilities and the gas pipeline junctions are modeled as nodes while the gas pipeline segments are described as links, with their representation in Fig.2. In addition, the gas storage facilities and the gas receipt facilities are regarded as source nodes, the connection points and gas compressors are modeled as transmission nodes and the gas delivery facilities as load nodes. Finally, there are 67 links and 63 nodes in total, with 14 source nodes, 23 transmission nodes and 26 load nodes. The capacity of each pipeline segment is set as $c \sim D^r$ with r =2.5 [35].

For the power system in Harris County, it includes the high voltage (35-345kv) transmission network and the low voltage (0.12-35kv) distribution networks. The transmission network has 551 transmission lines and 417 nodes, including 23 power plants and 394 substations, with its geographical representation shown in Fig. 2 [36]. All transmission substations are initially regarded as load nodes, with their load levels estimated proportionally to the number of households in that tract. For the distribution network, its information is not available for analysis due to security concerns. This paper assumes that all types of gas nodes require electricity to keep their normal operation, and

each gas node connects to its nearest transmission load substation. Note that these interdependent links from the power transmission network to gas system for power supply are a part of power distribution network; hence, for illustrative purpose, this paper models the power-to-gas interdependent links as the power distribution network, and other parts of the distribution network are not considered. Under these assumptions, the distribution network has 63 distribution load nodes, which connect with their nearest load substations by 63 distribution lines respectively. Each of these gas-depended transmission load substations is assumed to evenly distribute its load to its connected distribution load nodes. The above descriptions have established the interdependencies from the power system to the gas system. For simplification, this paper only considers this power-to-gas unidirectional interdependency.

2.2 Modeling of hazards and component fragilities

As the Harris County is located near the Gulf Coast, this paper mainly considers hurricane hazards to illustrate the proposed resilience assessment approach. This type of hazards can be described by a Poisson process of constant rate λ_h such that the time interval between two consecutive hurricane events has an exponential distribution [37]. The annual occurrence rate of hurricane hazards in Harris County with category 1 or higher is λ_h =1/7/year, and the probability of a hurricane belonging to each category given it occurs is respectively 0.53, 0.19, 0.15, 0.08, and 0.05 [23, 34]. The HAZUS-MH3 software is used to generate hurricane scenarios [38], each of them is grouped to a category and then finally there are 50 different scenarios for each category. Fig. 3 shows a generated hurricane scenario grouped into category 3.

To simulate hurricane hazards during a time period from 0 to T, an occurrence time is

first determined by adding a random value generated based on Eq. (3) to the last hurricane occurrence time or zero (if no hurricane has occurred before). If this time is less than T, generate a hurricane category according to the above hurricane category probabilities, and select a pre-generated hurricane scenario at random from the scenarios already grouped per category and then move to the next occurrence time until the time T.

Given a hurricane scenario, infrastructure component failure probabilities can be computed by their fragility models under wind loads. For the power system, power plants are mostly impervious to structural hurricane damage and then their fragilities are not considered; the fragilities and the repair times of other components, including transmission substations, transmission lines, distribution lines (or interdependent links) and distribution load nodes, are estimated based on models introduced in the reference [23]. For the gas system, underground pipelines are mostly invulnerable to wind hazards, and then only the gas node failures are considered according to their associated log-normal fragility curves, with median fragilities in the range of 60-72ms^{-1} depending on local terrain roughness [38-39]. Based on the HAZUS-MH3 data [38], the repair times for low, moderate, severe, complete damage levels of a gas node are set to satisfy normal distributions N(21.6h, 7.2h), N(74.4h, 64.8h), N(324h, 240h), N(840h, 432h),respectively.

2.3 Modeling of cascading failures within and across infrastructure systems

Under a hurricane scenario, component damage scenarios can be generated by comparing their failure probabilities to uniformly distributed random numbers within [0, 1]. Initial damaged components can trigger cascading failures within and across multiple systems. As this process lasts much shorter than the restoration process, this paper assumes the cascading failures are instantaneous as a first approximation.

For the case of unidirectional interdependencies from the power to the gas system, the cascading failures are simulated according to the following procedures: First, identify power system component failures directly from the event, and then check the system topology to record all unconnected sub-grids. For each sub-grid, its response is modeled according to the following rules: (1) If it does not contain any power plant, then all the load nodes are assumed failed (in terms of service); (2) If the sum of all power plant capacities is larger than the sum of the demand, then check the line flow constraints after running a DC power flow equation; if there are violations, cut the load to the load substation or load node with the smallest load level until the line constraints are satisfied; (3) If the sum of all power plant capacities is smaller than the sum of the demand, cut the load to the load substation or load node with the smallest load level first to balance the supply and the demand, and then run the step (2). The DC power flow equation $\boldsymbol{F} = \boldsymbol{AP}$ provides a relationship between power flow vector $\boldsymbol{F}$ consisting of the flow through each line and the power injection vector $\boldsymbol{P}$ at the nodes, with $\boldsymbol{A}$ as a constant matrix [40]. When the line flow constraints are satisfied, power grid component states and performance level can then be recorded and computed. Second, identify gas system component failures directly from the hurricane event and indirectly due to power system outage and then employ the maximum network flow model [35, 41] to estimate gas system performance, which is the maximum flow from the source nodes to the load nodes. Note that if there exist bi-directional interdependencies between two systems, the above two steps can be repeated to reach the steady states of both systems and then the steady-state system performance after the event can be computed.

2.4 **Modeling of multi-systems' joint restoration processes**

Immediately after a disruptive event, utility companies will next make restoration decisions and repair their systems to normal states. This paper models the restoration processes of interdependent systems by capturing two critical factors. The first factor is the mobilization of restoration resources. There are different types of resources for different types of restoration. To model resource quantities, this paper considers all resources with the same effectiveness, and one unit of restoration resources refers to a repair team, including repair crews, vehicles, equipment and some replacement components. Each damaged component needs one unit of restoration resources for recovery, and the repair times for different damaged components are set according to the probability distributions introduced in reference [23]. For simplification, this paper models the amount of restoration resources constant. But note that the amount of restoration resources could increase with time, and an increasing function can be used to characterize the dynamic process of resource mobilization.

The second factor is the restoration sequence. For a damage scenario, given the restoration resources, various restoration sequences might produce different restoration times and different impact areas under the event. The impact are is the area between the real performance curve and the targeted performance curve during the restoration period, and taking the performance curves in the Fig. 1 as an example, the impact area *IA* under the second event is computed by the following equation:

$$IA = \int_{t_0}^{t_E} [P_T(t) - P_R(t)]dt \tag{3}$$

According to the resilience definition, the less the impact area is, the larger the resilience value should be. Hence, this paper will optimize the restoration sequence to minimize the impact area under each damage scenario. This problem is difficult to solve with standard

optimization techniques because of the complicated cascading failure process within and across multiple systems. Instead, this paper uses the genetic algorithms, which are power stochastic search algorithms that have been successfully used in the literature to optimize restoration sequences of damaged components of single infrastructure systems after disruptive events [42-43].

Genetic algorithms (GA) simulate an evolutionary process with N individuals which represent points in a search space [44]. Every individual is encoded as a string called a genotype. In each step of a genetic algorithm, called a generation, each individual is evaluated by a relative fitness value with regard to the entire population. According to natural evolution, offsprings are produced by using three types of operators: selection, crossover and mutation. The selection operator chooses an individual with a probability depending on its fitness value. Two selected individuals produce two descendants by using the crossover operator which exchanges substrings of the codes of the two chosen individuals. Each descendant then generates an offspring by using the mutation operator, which changes the genotype of the descendant with a mutation probability. This paper applies a GA to optimize restoration sequence of damaged components of multiple systems. The procedures to search an optimum restoration sequence can be determined according to the following steps.

First, number damaged infrastructure components and express a restoration sequence by a genotype, which is a string composed of a line of those numbers. For example, when two nodes and two links are damaged and respectively numbered by 1, 2, 3, 4, and the restoration sequence is in the order of 1→2→3→4, a genotype for that process is then expressed by a string 1234 and the length of genotype is equal to the number of damaged

components. Genotypes of initial individuals are randomly generated.

Second, compute the fitness value of each genotype by using linear normalization technique. For each genotype, which corresponds to a restoration sequence, the restoration process is simulated according to the power and gas systems performance models, and then the impact area is computed. After calculating the impact areas for all produced genotypes, arrange them by the order starting with the smallest impact area. The fitness value of the i-th genotype is defined by $f(i)=\max(a-bi,1)$ [42], in which i is the order of the genotype, a is the maximum fitness value and b is the reducing ratio. This paper sets the value of a as 100, and b as 2.5.

Third, use the selection operator to choose superior genotypes according to their fitness values. This paper uses the roulette wheel selection technique: choose an uniformly distributed arbitrary number between 0 to the total sum of fitness values of all genotypes, make a cumulative sum of all fitness values to get a summing fitness value sequence, and then compare each element in this sequence with p, and select the genotype with its element in the summing fitness value sequence first exceeding p. This process is repeated until enough genotypes for the next generation is reached.

Forth, use the crossover operator to produce new individuals (or descendants). For a pair of genotypes (or two parents), if an uniformly distributed random number is less than crossover probability, then the crossover operator is made according to the following rules: a cutting point which is a random integer number between 1 to the genotype length, is selected randomly; the first descendant inherits a longer substring from the first parent and replace the genes of shorter substring in the order of genes appeared in the second parent. The second descendant inherits a longer substring from the second parent and

replaces the genes of shorter substring in the order of genes appeared in the first parent. For example, 12345678 and 37568241 are two genotypes, and assume a cutting point 5 is selected. Then the first descendant inherits the substring of 12345 from the first parent and the remaining substring of 678 is replaced by 768 which is the order of genes appeared in the second parent. Hence, the first descendant is 123456768, while the second descendant is 37568124.

Fifth, use the mutation operator to generate the next-generation individuals. For each descendant produced in forth step, two randomly selected genes of its string is replaced at a mutation probability. For example, assume 12345678 is a genotype, if a uniformly distributed random number between 0 and 1 is less than the mutation probability, and two genes 2 and 7 are selected, then the mutated genotype 17345628 is saved as an individual in next generation.

Sixth, return to the second step until the maximum generation is reached.

Based on the above procedures, this paper sets the number of individuals in each generation as 50, the maximum generation as a number which makes the best impact area in each generation converge and not fluctuate for more than 30 steps, the crossover probability as 0.5 and the mutation probability as 1.0. The genotype in the final generation with the minimum impact area corresponds to the optimum restoration sequence. Note that similar procedures above have been proved to work well to search the optimum restoration sequences of damaged components in single systems [42]. Hence, this paper does not discuss the effectiveness of this algorithm, but with the main focus to analyze how the interdependencies would affect the restoration processes as well as the resilience assessment. To investigate the effects due to the interdependencies, this paper

considers five types of restoration strategies for comparison purpose.

The first strategy is ***random restoration strategy*** RS_1, where power or gas damaged components are randomly selected to repair.

The second strategy is ***independent restoration strategy*** RS_2, where power and gas damaged components are repaired with the sequences to minimize each system's impact area respectively without considering interdependencies. This strategy uses the above GA to optimize the sequences of power and gas damaged components respectively.

The third strategy is ***power first and gas second restoration strategy*** RS_3, where power damaged components are first repaired with the sequence to minimize the IA_P, with known electricity-restored time of each gas node, gas damaged components are then repaired with the sequence to minimize the IA_G. This strategy first uses the above GA to optimize the sequences of power damaged components respectively, and then obtain all gas nodes' electricity-restored time, which is then used in another GA to optimize the sequences of gas damaged components.

The forth strategy is ***gas aimed restoration strategy*** RS_4, where power and gas damaged components are repaired with the sequences to minimize the IA_G without considering the IA_P. This strategy numbers the power and gas damaged components together, with the objective function as $0*IA_P+1*IA_G$.

The fifth strategy is ***power and gas compromised strategy*** RS_5, where power and gas damaged components are repaired with the sequences to minimize the evenly weighted sum (weight coefficients as 0.5 and 0.5) of IA_P and IA_G. This strategy numbers the power and gas damaged components together, with the objective function as $0.5*IA_P+0.5*IA_G$.

3. Simulation Results

The proposed framework includes many models, such as the hurricane generation model, component fragility models, system performance models, cascading failures model across multiple systems, restoration models, and so on. Due to lack of sufficient data, this paper cannot provide an overall validation analysis of all these models, but note that some of these models have been validated in previous separated references. For example, the gas system performance can be approximated well by the maximum network flow model [35], while the power system component fragilities model under hurricane events, the DC power flow based performance model and some parts of the power system restoration models have been tested to work well in another reference [23].

As this paper focuses on resilience contribution analysis of different joint restoration strategies, this section will use the proposed framework to design simulations to mainly analyze the restoration processes of the two systems under typical hurricane scenarios (section 3.1), and compare the resilience effectiveness of different restoration strategies (section 3.2). In addition, different metrics can be used to quantify system performance levels, and then produce various dimensions of system resilience. Taking power systems as an example, the metrics could be the percentage of power supply, the percentage of critical facilities with power, and the percentage of customers with power, which correspond to technical, organizational and social dimensions of resilience. A multi-dimensional resilience assessment and analysis of the power system in Harris County is provided in another reference [23]. This paper mainly focuses on the illustration of multi-systems' resilience assessment approach, and then only considers the technical dimension of resilience. The percentage of power supply in its normal value for the power system and the percentage of maximum gas flow in its normal value for the gas system are used

as the performance metrics for technical resilience assessment.

3.1 Restoration processes for typical hurricane scenarios

For a hurricane scenario shown in Fig. 3, it can generate many damage scenarios, and then the average restoration curve over various scenarios is used to describe system restoration process under the event. For the hurricane scenario shown in Fig. 3, when the amount of restoration resources is r_p=10 units for the power system, and r_g=1 unit for the gas system, the average power and gas restoration curves over 200 damage scenarios are depicted in the Fig. 4 for different restoration strategies. The number of damage scenarios set in the simulation is selected to make the average impact areas converge to a deviation of less than 0.1% under all restoration strategies.

From the figures, under various strategies, the time for complete restoration is 82 days for the power system, and 140 days for the gas system. For the independent strategy RS_2 and the power first and gas second strategy RS_3, their curves are overlapped for the power system because this paper only considers un-directional power-to-gas interdependencies so that these two strategies are actually the same for the power system; compared with the RS_2, the RS_3 improves the gas restoration process, with IA_G decreasing from 46.7 to 42.7. Also, the random strategy RS_1 is the worst for both systems, and the gas aimed strategy RS_4 makes the gas restoration curve the best, but note that the power restoration curve under this strategy is still better than the random strategy RS_1, which indicates that the power system also gets benefits when its restoration sequence is optimized to minimize the gas impact area. This is mainly because optimizing gas restoration sequences makes damaged power components in the path of connecting power plants to gas-depended power load nodes have the highest repair priorities, and

then produces less power impact area than the random strategy RS_1. In addition, compared to the gas aimed strategy RS_4, the power and gas compromised strategy RS_5 improves the power restoration process effectively, with IA_P decreased from 19.1 to 12.0, but for the gas system, the improvement is not much, with IA_G decreased from 31.2 to 30.0. This is mainly because current restoration resources' settings make the gas impact area much larger than power impact area, and then the evenly weighed sum of power and gas impact areas as the objective function for RS_5 will return the minimum gas impact area close to that from RS_4.

The above results are based on a typical hurricane event. Whether similar results could be found for other hurricanes with various intensities? To investigate this question, this paper selects some other hurricanes with different average peak wind gusts ranging from 76 to 156 mph, and simulates their expected power and gas impact areas under various restoration strategies, with the results shown in Fig. 5. The simulation times under different hurricanes vary differently from 200 to 1000 so that the average impact areas are converged to a deviation of less than 0.1% under all strategies. Note that for different hurricanes, the restoration resources are still fixed as r_p=10 units for the power system and r_g=1 unit for the gas system. From the figures, under different hurricane intensities, the random strategy RS_1 always generates the largest impact areas for both systems, while the independent strategy RS_2 and the power first and gas second strategy RS_3 always produce the least IA_P, and the gas-aimed strategy RS_4 always brings the minimum IA_G. In addition, for small-intensity hurricanes with a few damaged components, different restoration strategies produce almost identical impact areas; for large-intensity hurricanes with large-scale damaged components, the expected power or

gas impact areas under various strategies show larger and larger differences as the intensity increases. These results indicate that when interdependent systems are subjected to large-scale damage, under limited restoration resources, the scheduling of restoration tasks is very crucial for systems' recovery performance.

3.2 Hurricane resilience assessment

When the restoration resources are fixed as r_p=10 units for the power system and r_g=1 unit for the gas system under different hurricane scenarios, set the time period T=100 years to capture hurricanes with categories 4-5, and run the simulation 100,000 times so that the average resilience values all converge to less than 0.1%, with results listed in Table 1.

Table 1: Expected resilience values of power and gas systems under various restoration strategies, the evenly weighted sum of two systems' resilience are also displayed as the total resilience of both systems. The restoration resources are fixed as 10 units for the power system and 1 unit for the gas system under different hurricane events.

System	RS_1	RS_2	RS_3	RS_4	RS_5
Power System	0.9892	0.9944	0.9944	0.9904	0.9929
Gas System	0.9833	0.9864	0.9868	0.9910	0.9906
Both Systems	0.9862	0.9904	0.9906	0.9907	0.9918

From the table, it can be found that for the power system, the independent strategy RS_2 and the power first and gas second strategy RS_3 both are the best, while the random strategy RS_1 is the worst, and the gas aimed strategy RS_4 is still better than RS_1 and produces a higher power system resilience; for the gas system, its resilience value is

always less then power system resilience, with the gas aimed strategy RS_4 producing the best resilience and the power and gas compromised strategy RS_5 generating a little smaller resilience value than RS_4, while the strategy RS_3 produces the resilience value with 0.004 higher than RS_2. Although this difference value seems very small, the saved economic losses might be millions of dollar per year [23]. In addition, if quantifying the total resilience of both power and gas systems as the evenly weighed (weight coefficients are both 0.5) sum of individual system resilience, the results are also shown in Table 1. It can be found that the power and gas compromised strategy RS_5 produces the largest total resilience, while the random strategy RS_1 is still the worst one. Note that depending on the resilience weight coefficients assigned to each system, the total resilience value as well as the best restoration strategy might be varied. When the power system resilience weight coefficient is larger than 0.72, the power first and gas second strategy RS_3 is the best; when the power system resilience weight coefficient is larger than 0.18 but less than 0.72, the power and gas compromised strategy RS_5 is the best; when the power system resilience weight coefficient is less than 0.18, the gas-aimed strategy RS_4 is the best. Note that all these best restoration strategies have considered the interdependencies, which means considering infrastructure interdependencies during restoration decision makings is crucially important for resilience enhancement of interdependent systems.

The above results are based on T=100 years and focus on the expected resilience value. Whether similar results can be obtained for other values of T? Equation (2) provides a positive answer to this question. To further validate it, this paper selects two other values T=10 years and T=50 years to run the simulation 1000,000 times and 200,000 times respectively. The obtained expected power and gas resilience values are

identical with those shown in table 1. But their resilience probability distributions under different values of T vary largely. The resilience distribution results under the strategy RS_5 are shown in Fig. 6. To clearly show these curves in the same plot, the resilience $R(T)$ is shown in a logarithmic form $-\log_{10}(1-R(T))$. From the figures, the larger the T value is, the larger probability a high power or gas resilience value can be reached. When T=10 years, there is a probability of 0.25 at which the resilience value is equal to 1.0.

Also, the quantities of restoration resources affect system resilience. To investigate their relationships, this paper sets several other values of r_p while r_g is fixed as 1 unit, and then estimates the power and gas expected resilience as a function of r_p, with the results shown in Fig. 7. From the figures, it can be found that under limited restoration resources (small r_p), various restoration strategies lead to largely different resilience values, where the random strategy RS_1 produces the least resilience for both two systems, the independent strategy RS_2 and the power first and gas second strategy RS_3 both generates the largest resilience for the power system, while the gas aimed strategy RS_4 is the best for the gas system, with the power and gas compromised strategy RS_5 only a few worse than RS_4. Also, with the increase of r_p the five restoration strategies produces closer and closer resilience value for the power system; and for the gas system, the strategies RS_3, RS_4 and RS_5, which all consider the interdependencies, finally produce almost identical resilience values under large r_p. This is because under large r_p various power restoration strategies will produce the same power impact area as well as identical electricity-restored time for gas nodes, then the strategies RS_3, RS_4 and RS_5 actually have the same optimization objective, which is to minimize the gas impact area, hence for sufficient power restoration resources gas impact areas under these three strategies are identical,

which then lead to identical resilience values. When the amount of gas restoration resources r_g increases, similar results are found and all restoration strategies, including the random strategy RS_1, produce closer and closer expected gas resilience until completely identical.

4. Discussions and Conclusions

Disaster-resilient cities or communities largely depend on the resilience of their infrastructure systems, which are not alone but interdependent. This paper adapts an existing resilience framework for single systems to interdependent systems. As some steps of the proposed framework have been studied for interdependent system vulnerability, this paper mainly focuses on the modeling of multi-systems' joint restoration processes to support resilience assessment. Taking the interdependent power and gas systems in Harris County, Texas under hurricane hazards as an example, five joint restoration strategies have been introduced to analyze their technical resilience contribution. Results shows that under limited restoration resources, the random restoration strategy RS_1 produces the least resilience for both two systems, the independent restoration strategy RS_2 and the power first and gas second restoration strategy RS_3 both generates the largest resilience for the power system, while the gas aimed restoration strategy RS_4 is the best for the gas system; and if quantifying the total resilience of both systems as the evenly weighted sum of individual system resilience, the power and gas compromised restoration strategy RS_5 is the best.

This paper not only provides a framework to assess interdependent systems' resilience, but also introduces a method to help utility companies search optimum joint restoration sequences of post-disaster interdependent systems, which is an effective strategy for rapid

restoration and infrastructure resilience enhancement. Note that for illustrative purpose, this paper only considers technical resilience, but the framework can be easily extended to consider organizational, social and economic resilience when other metrics are taken to measure system performance levels [23]. In addition, when applying the proposed framework to other systems, it requires changing some system parameter values, such as hazard type and return periods, component fragility curves for the specific hazard type, system property data, flow-related data, interdependent relationships, amount of resources and their mobilization rate, among others, but the main procedures and methods for resilience assessment are similar. Also, this paper only considers unidirectional interdependencies between systems, addressing bi-interdependencies and analyzing their impacts on multi-systems' restoration processes and resilience assessment are more interesting and will be our future research directions. Finally, collecting more sufficient data for overall validation of the framework, identifying possible resilience-based improvement strategies, such as the installation of backup power generators, and analyzing their effectiveness from a life-cycle cost-benefit perspective are also interesting topics in the field of resilience engineering.

Acknowledgements

This material is based upon work supported in part by the National Science Foundation of China under Grant 51208223, and the Fundamental Research Funds for the Central Universities under Grant 2014QN166. Any opinions, findings, and conclusions or recommendations expressed in this material are those of the authors and do not necessarily reflect the views of the sponsors.

References

[1] Burby RJ, Beatley T, Berke PR, Deyle RE, French SP, Godschalk DR, Kaiser EJ, Kartez JD, May PJ, Olshansky R, Paterson RG, Platt RH. Unleashing the power of planning in creating disaster-resilient communities. Journal of the American Planning Association, 1999; 65(3):247–258.

[2] Godschalk DR. Urban hazard mitigation: Creating resilient cities. Natural Hazards Review, 2003; 4(3):136–143.

[3] United Nations International Strategy for Disaster Reduction (UN/ISDR). Hyogo Framework for Action 2005–2015: Building the Resilience of Nations and Communities to Disasters. Geneva, Report No.: UN/ISDR-07-2007-Geneva.

[4] Berke PR, Campanella TJ. Planning for postdisaster resiliency. Annals of the American Academy of Political and Social Science, 2006; 604(1):192–207.

[5] Rinalidi S.M., Peerenboom J.P., and Kelly T. (2001). Identifying, understanding and analyzing critical infrastructure interdependencies. IEEE control system magazine, December, 11-25.

[6] Peerenboom J.P., Fisher R.E., Rinaldi S.M. and Kelly T.K. (2002). Studying the chain reaction. Electric Perspectives 27(1), 22-35.

[7] Robert B., Senay M.H,, Plamondon M.E.P. and Sabourin J.P. (2003). Characterization and ranking of links connecting life support networks. Public safety and emergency preparedness Canada. Ontario.

[8] Plodinec M.J. Definitions of resilience: an analysis. Community and Regional Resilience Institute*;* 2009. *p.* 1-17. http://www.resilientus.org /library/CARRI_Definitions_Dec_2009_ 1262802355.pdf.

[9] Francis R. and Bekera B. A metric and framework for resilience analysis of engineered and infrastructure systems. Reliability Engineering and System Safety. http://dx.doi.org/10.1016/j.ress.2013.07.004

[10] The Infrastructure Security Partnership (TISP)—Regional disaster resilience: a guide for developing an action plan (2011 edition). http://www. tisp.org/tisp/file/Template_TISP%20Layout_v29%282%29.pdf

[11] Commonwealth of Australia. Critical infrastructure resilience strategy. Canberra: Commonwealth of Australia; 2010. http://www.emergency.qld.gov.au/ publications/pdf/Critical_Infrastructure_Resilience_Strategy.pdf

[12] NIAC, National Infrastructure Advisory Council—a framework for establishing critical infrastructure resilience goals final report and recommendations; 2009. http://www.dhs.gov/xlibrary/assets/niac/niac-a-framework-for-establishing-critical-infrastructure-resilience-goals-2010-10-19.pdf

[13] Bruneau, M., Chang, S.E., Eguchi, R.T., Lee, G.C., O'Rourke, T.D., Reinhorn, A.M., Shinozuka, M., Tierney, K., Wallace, W.A., and Winterfeldt, D.V. A Framework to Quantitatively Assess and Enhance the Seismic Resilience of Communities. Earthquake Spectra. 2003, 19(4):733–752.

[14] Bruneau, M., Reinhorn, A.M. Exploring the concept of seismic resilience for acute care facilities. Earthquake Spectra. 2007, 23(1):41–62.

[15] Chang, S.E., Shinozuka, M. Measuring improvements in the disaster resilience of communities. Earthquake Spectra. 2004, 20(3):739-755.

[16] Cimellaro, G., Reinhorn, A., Bruneau, M. Framework for analytical quantification of disaster resilience. Engineering Structures. 2010, 32: 3639-3649.
[17] Reed, D.A., Kapur, K.C. and Christie, R.D. Methodology for assessing the resilience of networked infrastructure. IEEE system journal. 2009, 3(2):174-180.
[18] Vugrin, E.D., Warren, D.E., Ehlen, M.A. and Camphouse, R.C. A framework for assessing the resilience of infrastructure and economic systems, in Sustainable and Resilient Critical Infrastructure Systems: Simulation, Modeling, and Intelligent Engineering, Kasthurirangan Gopalakrishnan and Srinivas Peeta, eds., Springer-Verlag, Inc.. 2010.
[19] Zobel, C.W. Representing perceived tradeoffs in defining disaster resilience. Decision support systems. 2010, 50: 394-403.
[20] Barker K., Ramirez-Marquez J.E., Rocco C.M. Resilience-based network component importance measures. Reliability Engineering and System Safety 2013, 89-97.
[21] Henry D. and Ramirez-Marquez J.E. Generic metrics and quantitative approaches for system resilience as a function of time. Reliability engineering and system safety 2012: 114-122.
[22] Ouyang, M. and Duenas-Osorio, L. A three-stage resilience analysis framework for urban infrastructure systems. Structural Safety. 2012, 36: 23-31.
[23] Ouyang, M. and Dueñas-Osorio, L. Multi-dimensional hurricane resilience assessment of electric power systems. Structural Safety 2014, 48: 15-24.
[24] Ouyang, M. and Dueñas-Osorio, L. Time-dependent Resilience Assessment and Improvement of Urban Infrastructure Systems. Chaos, 2012, 22(3): 033122-033122-11.
[25] Ouyang M. Review on modeling and simulation of interdependent critical infrastructure systems. Reliability Engineering and System Safety 2014, 121, 43-60.
[26] Lian C. Y. and Haimes Y. Y. (2006). Managing the risk of terrorism to interdependent infrastructure systems through the dynamic inoperability input-output model. Systems Engineering 9(3): 241-258.
[27] Haimes Y. Y, Horowitz B. M., Lambert J. H., Santos J. R., Lian C. and Crowther K. G. (2005a). Inoperability input-output model for interdependent infrastructure sectors. I: Theory and methodology. Journal of Infrastructure Systems 11(2): 67-79.
[28] Lee E. E., Mitchell J. E. and Wallace W. A. (2007). Restoration of services in interdependent infrastructure systems: a network flows approach. IEEE Transactions on systems, man, and cybernetics—part C: application and reviews 37(6): 1303-1317.
[29] Wallace W. A., Mendonca D. M., Lee E. E., Mitchell J. E. and Chow Wallace J. H. (2003). Managing disruptions to critical interdependent infrastructures in the context of the 2001World Trade Center attack. In Beyond September 11th: An Account of Post-Disaster Research, special publication #39, J. L. Monday, Ed. Boulder, CO: Natural Hazards Research and Applications Information Center, Univ. of Colorado, 2003, pp. 165–198.
[30] Ouyang M. Comparisons of purely topological model, betweenness based model and direct current power flow model to analyze power grid vulnerability. Chaos. 2013, 23, 023114.

[31] Ouyang M. Zhao L., Pan Z. and Hong L. Comparisons of complex network based models and direct current power flow model to analyze power grid vulnerability under intentional attacks. Physica A. 2014, 45-53.
[32] Coffrin C., Hentenryck P.V., Bent R. Last-mile restoration for multiple interdependent infrastructures. Proceedings of the Twenty-sixth AAAI conference on Artificial Intelligence. 2012. Toronto, Ontario, Canada at the Sheraton Centre Toronto, from July 22–26, 2012.
[33] Platts. Topology of the State of Texas power transmission network; 2009. [accessed 05/2009] http://www.platts.com/.
[34] Ouyang, M. and Dueñas-Osorio, L. An approach to design interface topologies across interdependent urban infrastructure systems. Reliability engineering and system safety. 2011, 96(11): 1462-1473.
[35] Carvalho R., Buzna L., Bono F., Gutierrez E., Just W. and Arrowsmith D. Robustness of trans-European gas networks. Physical Review E, 2009, 80: 016106.
[36] Bayliss, C. and Hardy, B. Transmission and distribution electrical engineering. Third Edition. Elsevier Ltd. 2007.
[37] Quanta Technology, Undergrounding Assessment Phase 3 Final Report: Ex Ante Cost and Benefit Modeling. Prepared for the Florida Electric Utilities and submitted to the Florida Public Service Commission per order PSC-06-0351-PAA-EI, May 2008.
[38] Federal Emergency Management Agency. Hazards U.S. Multi-Hazard (HAZUS-MH) Assessment Tool v1.3. www.fema.gov/plan/prevent/hazus/index.shtm. 2011.
[39] Sanks R., Tchobanoglous G., Jones G. and Bosserman B. Pumping station design. Butterworth-Heinemann, 3rd edition.2008.
[40] Dobson, I., Carreras, B.A., Lynch, V.E., and Newman, D.E. Complex systems analysis of series of blackouts: cascading failure, critical points and self-organization. Chaos. 2007, 17(2):026103.
[41] Monforti F and Szikszai A. A monte-carlo approach for assessing the adequacy of the European gas transmission system under supply crisis conditions. Energy policy 2010; 38(5):2486-2498.
[42] Sato T. and Ichii K. Optimization of post-earthquake restoration of lifeline networks using genetic algorithms. Proceedings of the 6th U.S.–Japan Workshop on Earthquake Disaster Prevention for Lifeline Systems, Osaka City, Japan, 1995.
[43] Xu N., Guikema S.D., Davidson R.A., Nozick L.K., Cagnan Z. and Vaziri K. Optimizing scheduling of post-earthquake electric power restoration tasks. Earthquake engineering and structural dynamics 2007; 36: 265-284.
[44] Davis L. handbooks of genetic algorithms, Van Nostrand Reinhold, 1991.

Research Highlights

- We propose a method to assess resilience of interdependent infrastructure systems.
- We consider unidirectional interdependencies from power system to gas system.
- Multi-systems' restoration processes are solved by using genetic algorithm.
- Effectiveness of five restoration strategies are compared and analyzed.
- Interdependency-based strategies produce the largest total resilience.

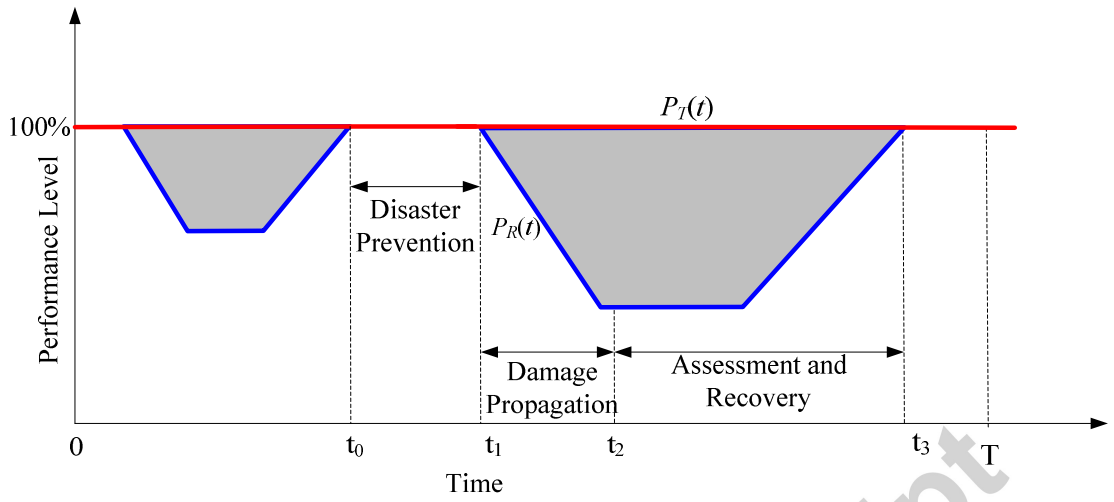

Fig.1: Typical performance process of an infrastructure system during a time period T with several disruptive events (adapted from the reference [22]).

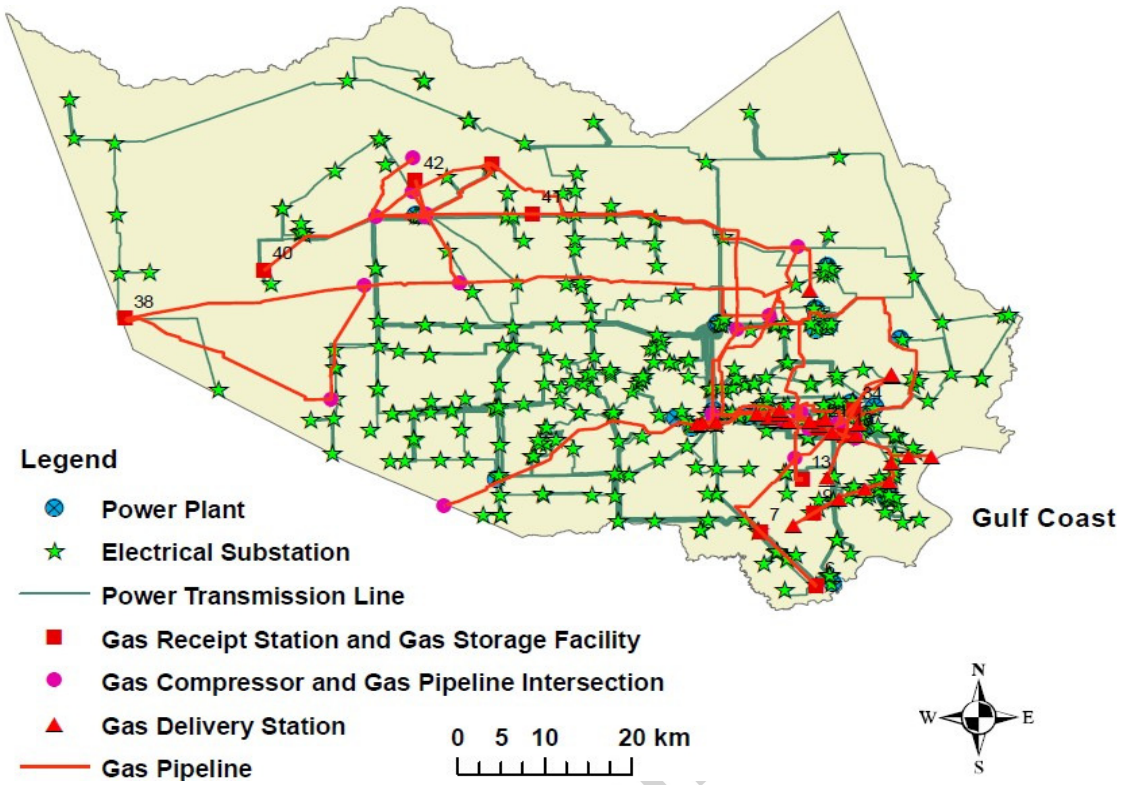

Fig.2: A geographical representation of power and gas systems in Harris County, Texas (excerpted from the reference [34]).

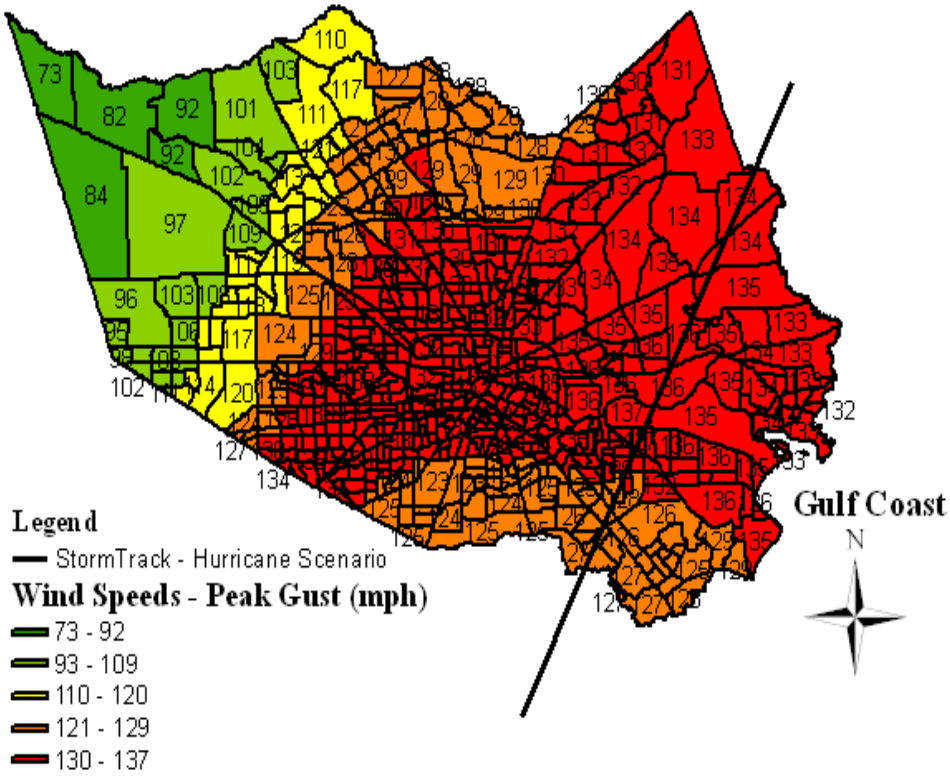

Fig.3: A hurricane scenario in Harris County grouped into category 3 (excerpted from the reference [23], note that the wind speeds in the map are peak wind gusts, while the hurricane category is grouped based on sustained wind speed, the former is assumed equal to the latter multiplied by 1.08 to group hurricane scenarios into some category).

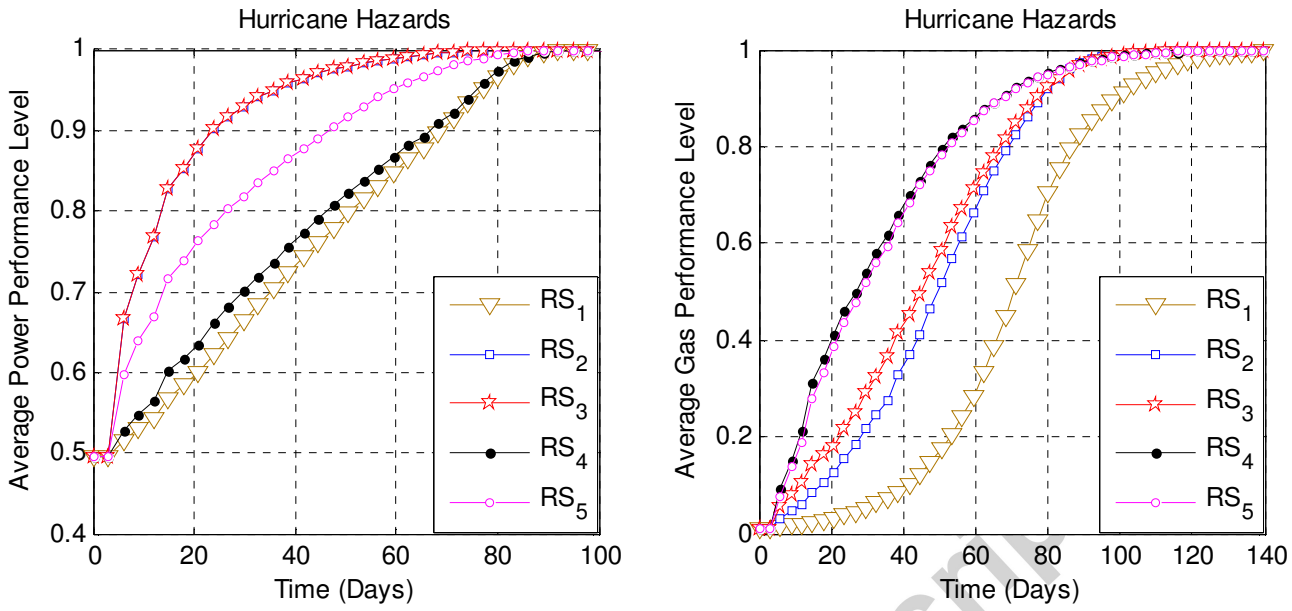

(*a*) (*b*)

Fig. 4: Average restoration curves of the power and gas systems in Harris County, Texas, USA under the hurricane scenario shown in Fig. 3. The results are averaged over 200 damage scenarios. The restoration resources are 10 units for the power system and 1 unit for the gas system. (*a*) power system; (*b*) gas system.

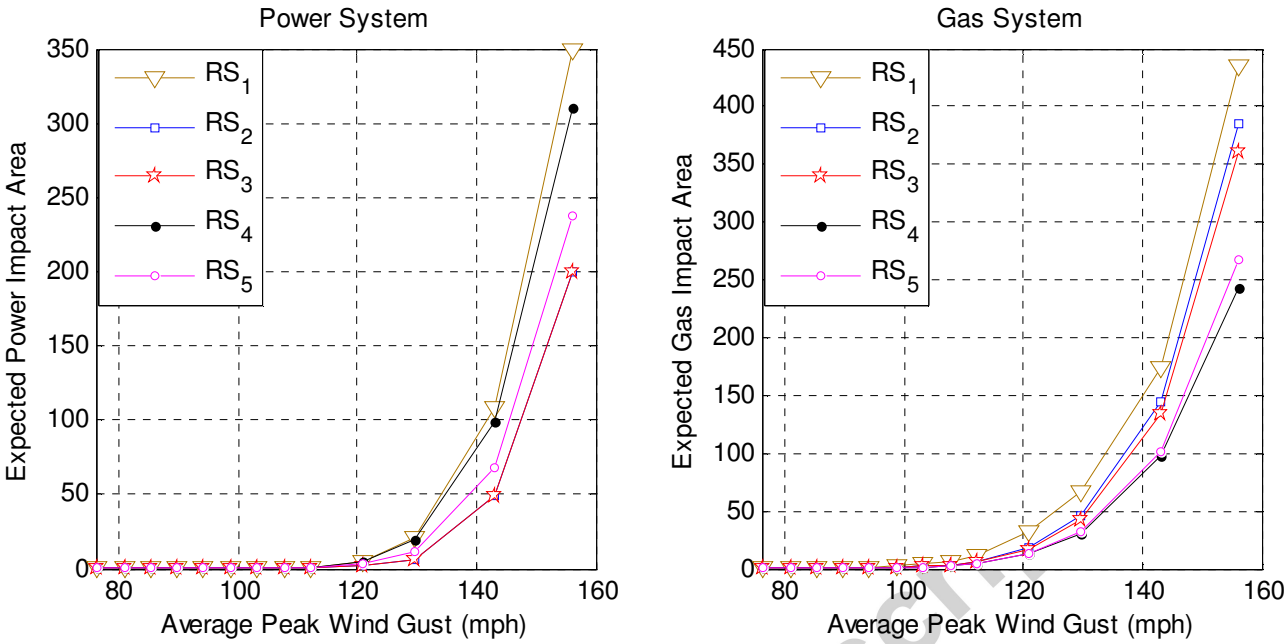

(*a*) (*b*)

Fig. 5: Expected power and gas impact areas under hurricane scenarios with various average peak wind gusts. The restoration resources are fixed as 10 units for the power system and 1 unit for the gas system. (*a*) power system; (*b*) gas system.

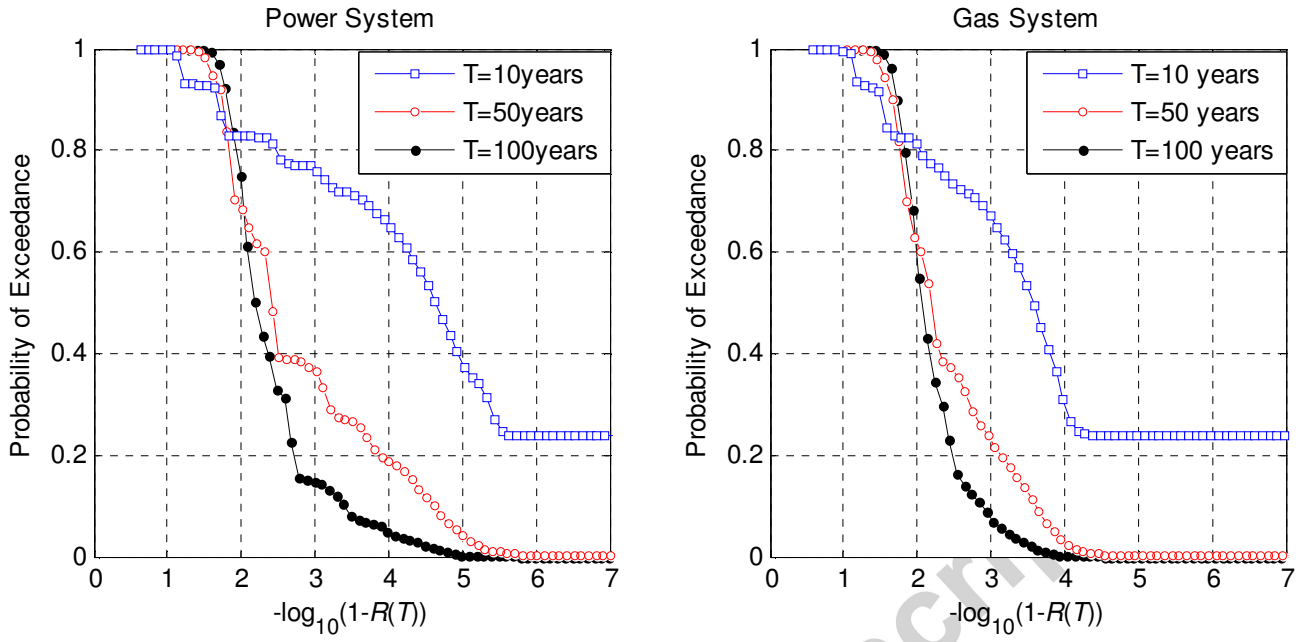

(*a*) (*b*)

Fig. 6: Probabilistic distribution of resilience $R(T)$ under different values of T for power and gas systems under the restoration strategy RS_5. The resilience $R(T)$ is shown in a logarithmic form $-\log_{10}(1-R(T))$, where $-\log_{10}(1-R(T))=2$ means $R(T)=0.99$, $-\log_{10}(1-R(T))=3$ means $R(T)=0.999$, $-\log_{10}(1-R(T))=4$ means $R(T)=0.9999$ ad infinitum. (a) power system; (b) gas system.

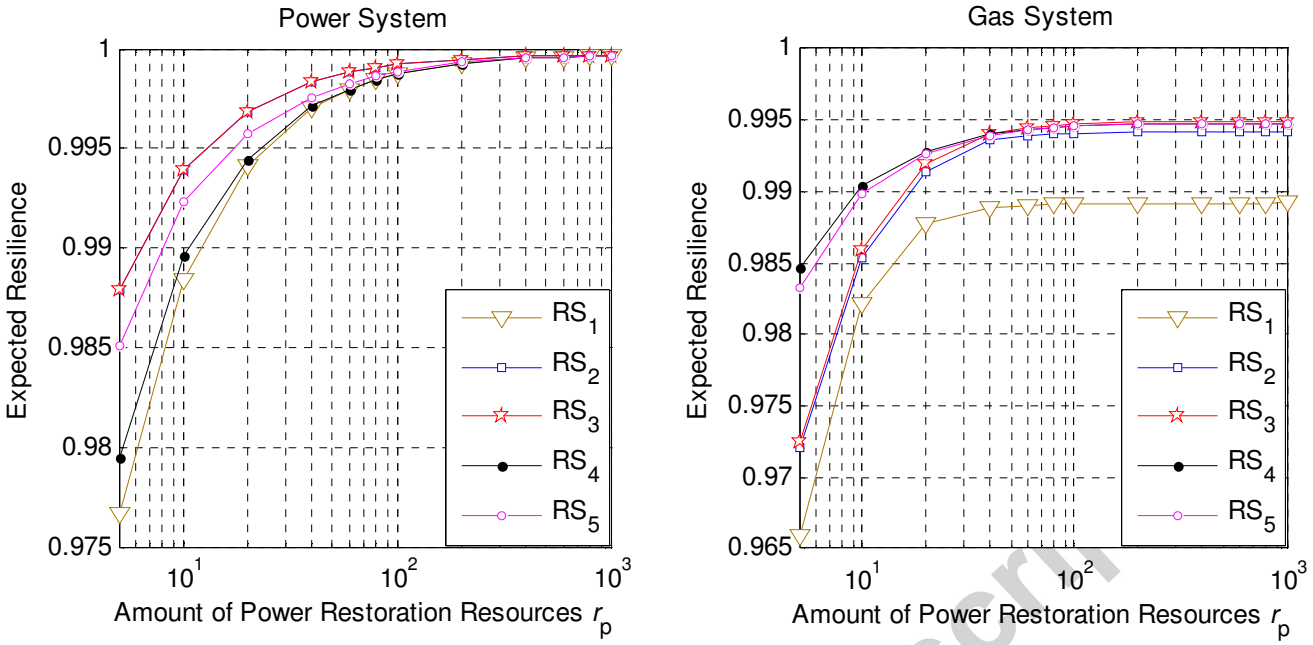

(*a*) (*b*)

Fig. 7: Expected power and gas resilience values as a function of power restoration resources r_p under the hurricane scenario shown in Fig. 3. The amount of gas restoration resources is fixed as one unit. (*a*) power system; (*b*) gas system.